Available online at www.eccomasproceedia.org
Eccomas Proceedia COMPDYN (2021) 4091-4099

ECCOMAS
Proceedia

COMPDYN 2021
8th ECCOMAS Thematic Conference on
Computational Methods in Structural Dynamics and Earthquake Engineering
M. Papadrakakis, M. Fragiadakis (eds.)
Streamed from Athens, Greece, 28 - 30 June 2021

NUMERICAL INVESTIGATION OF RUBBER BEARINGS WITH LOW SHAPE FACTOR UNDER SEISMIC EXCITATION

A. Orfeo[1], E. Tubaldi[1], A. Muhr[2], D. Losanno[3]

[1] Department of Civil and Environmental Engineering, University of Strathclyde
Glasgow, UK
{alessandra.orfeo, enrico.tubaldi}@strath.ac.uk

[2] Tun Abdul Razak Research Centre-TARRC
Hertford, UK
amuhr@tarrc.co.uk

[3] Department of Structures for Engineering and Architecture, University of Naples Federico II
Napoli, Italy
daniele.losanno@unina.it

Abstract

This study illustrates the development of a modeling strategy for simulating the seismic response of structures mounted on elastomeric bearings with a low shape factor (LSF). These bearings can be employed to achieve a three-dimensional seismic isolation of structures, due to their low vertical and horizontal stiffness. The first part of this work investigates the mechanical behaviour of LSF bearings by means of three-dimensional Finite Element (FE) analysis in Abaqus. The FE results provide a numerical evaluation of the horizontal, vertical, and rotational stiffness of the bearings. These are used in the second part of the study to develop in SAP2000 a simplified model of a structure with LSF bearings tested experimentally on the shaking table at University of Naples Federico II. The study results show that the developed model can be effectively used to simulate the response of the isolated structure under different earthquake inputs.

Keywords: Isolation system, low shape factor bearing, FE simulation, hyperelastic material.

ISSN:2623-3347
Peer-review under responsibility of the organizing committee of COMPDYN 2021.
doi: 10.7712/120121.8769.19344

1 INTRODUCTION

Elastomeric bearings are among the most common types of isolation system for protecting structures from earthquakes. They consist of multiple layers of rubber vulcanized to steel reinforcing layers that produce a combination of vertical stiffness and horizontal flexibility [1]. The geometry of these bearing is characterized by the primary shape factor, S, which defines the ratio of the loaded area to the area free to bulge for an individual rubber layer [2]–[4]. Shape factor values of 10-20 are typically used to guarantee high critical load capacities while keeping a low horizontal stiffness. On the other hand, bearings with high S values are significantly heavy due to the large number of steel plates and consequently expensive in terms of production and installation. Moreover, superstructures isolated with high vertical stiffness bearings are characterized by low vibration periods in the vertical direction, causing problems for critical facilities such as nuclear power plants or hospitals hosting sensitive equipment needing protection against the effects of vertical component of earthquake inputs.

The concept of low shape factor (LSF) rubber bearings as a way to achieve an economic 3D isolation has been investigated by other researchers [5] [6]. Recently, it has also been the object of an extensive experimental campaign carried out by Cilento et al. [7] to demonstrate the effectiveness of isolating a structure with a very LSF.

The aim of this paper is to present a finite element (FE) modelling strategy for simulating the seismic response of structures equipped with LSF bearings. The proposed strategy is validated considering the results of the experimental campaign carried out by Tun Abdul Razak Research Center (TARRC) and University of Naples Federico II on a structural prototype with LSF rubber bearings made with lightly filled natural rubber [8]. The first part of the paper focuses on the simulation of the bearing behaviour in Abaqus [9], using a three-dimensional modelling approach for the LSF bearings, with a hyperelastic constitutive law for the rubber calibrated using the double shear test results. In the second part of the paper, a simplified model based on a linearized description of the bearing mechanical behaviour is developed in SAP2000 [10]. This model is validated by simulating the shaking table tests performed on a structure isolated with LSF bearings. The numerical results of the analyses shed light on the possibility of using simplified device models for the preliminary seismic assessment of isolated structures mounted on LSF bearings.

2 NUMERICAL SIMULATIONS OF MATERIAL AND BEARING TESTS

This section describes the three-dimensional (3D) numerical models developed in Abaqus [9] to simulate the tests on the double shear testpieces and the elastomeric bearings carried out at TARRC [7]. The double shear cylindrical testpieces consisted of two rubber layers bonded to metal parts, as shown in Figure 1a, and were subjected to sinusoidal shear displacement histories. Figure 1b illustrates the laminated bearing considered in the test, which consists of three layers of rubber 19mm thick and sides 100x100 mm, designed to achieve a shape factor $S = 1.32$. The bearing was subjected simultaneously to static compression and dynamic shear loading in a double shear configuration. The testing sequence consisted of two cycles of sinusoidal displacement at increasing shear strain amplitudes [8] [11].

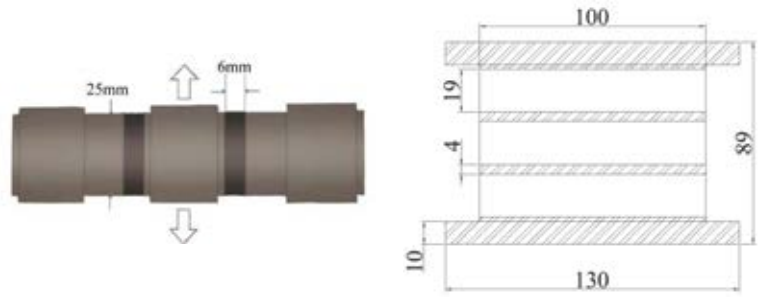

(a) (b)

Figure 1: (a) Double shear test piece geometry, (b) Elastomeric bearing geometry

In the numerical models, the rubber is described using a hyperelastic constitutive material. Hyperelastic materials are defined by the strain energy potential W, the strain energy stored in the material per unit of reference volume, as a function of the strain at that point in the material. Yeoh constitutive relationship is used in this study and the strain energy potential is derived from the reduced polynomial strain energy potential that is a function of only the deviatoric strain invariant I_1 and has the following expression:

$$W = \sum_{i=1}^{N} C_{i0} \left(I_1 - 3 \right)^i \tag{1}$$

where C_{i0} are material parameters. The Yeoh form is obtained for a number of terms N equal to 3. The values of material parameters C_{i0} in the equation (1) can be obtained from the double shear experiments and are shown in Table 1.

Model parameters	C10 [MPa]	C20 [MPa]	C30 [MPa]
Yeoh	0.3	-0.005	0.000311

Table 1 Material parameters for Yeoh hyperelastic material model

Rayleigh damping is used in the numerical analysis to describe the damping property of the rubber material. The coefficients for the Rayleigh damping are calculated using a damping ratio of 1% for the first and second modes of the isolated system described in section 3. The coefficient α for the mass matrix and the coefficient β for the elastic initial stiffness matrix are calculated to be 0.067926 and 0.00080, respectively.

The shear stiffness values obtained numerically for different maximum shear strain have been compared with the experimental data, as shown in Figure 2a. A good agreement between simulations and the test is found for all the investigated shear deformation amplitudes, apart from low values of shear strains.

The estimates of the equivalent damping ratio of the rubber block from FE analysis results for different levels of strain amplitude are shown in Figure 2b, where they are compared with the corresponding values obtained experimentally. Although a simple description of the damping is used, a good agreement is found between numerical and experimental results. It is noteworthy that more advanced description of the damping, e.g. using a Prony series approach [13] or the Bergstrom Boyce model [14], would require further tests in order to calibrate the higher number of model parameters.

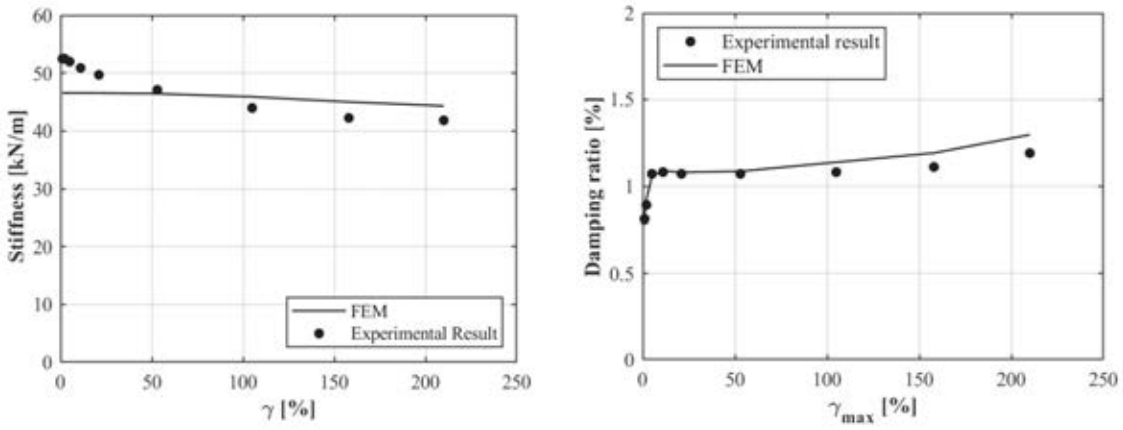

(a) (b)

Figure 2: Experimental and numerical values of (a) Shear stiffness for different maximum shear strains (b) Equivalent damping ratio for different maximum shear strains

The LSF bearing FEM model is illustrated in Figure 3. The rubber layers, the intermediate steel shim plates and end plates are modelled using C3D8H elements that are available in the Abaqus library [9]. The tie contact between steel and rubber layers of the bearing is expressed by contact pair option available in Abaqus. The displacement boundary conditions are applied to the top end plate while performing compression and shearing tests, whereas the bottom anchor plate is fixed in all degrees of freedom.

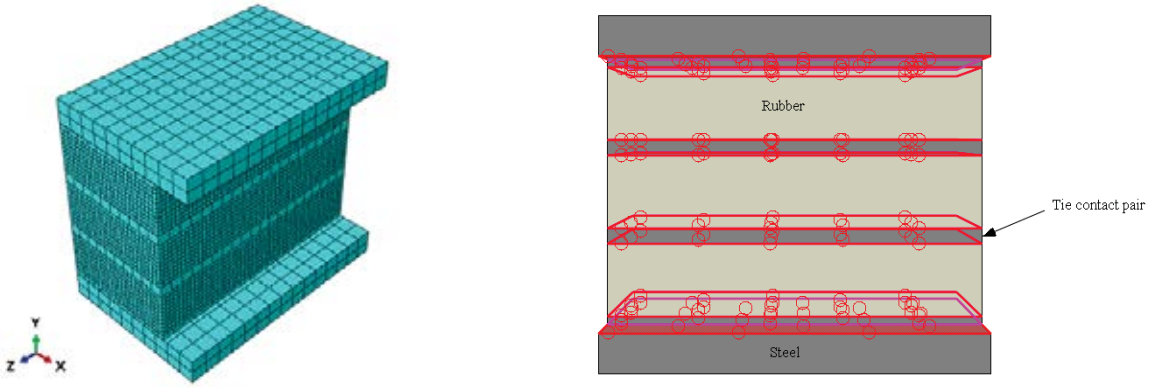

(a) (b)

Figure 3: Elastomeric Bearing: (a) Meshing, (b) Details of connections between various layers.

A vertical downward displacement was first imposed at the top plate, until a compressive load of 19kN is achieved, being the gravity load in the shaking table tests, described in the next section. Subsequently, two cycles of sinusoidal displacements are applied while preventing vertical motion and rotation of the top plate.

Figure 4a shows the changes with the maximum amplitude of average shear deformation of the horizontal secant stiffness of the bearing. These have been evaluated both numerically and experimentally as the ratio of base shear force to the maximum displacement at each incremental step. In general, the experimental and numerical values are very close, except for low shear strains, for which the numerical model is more flexible. The bearing equivalent viscous damping has been evaluated numerically and compared with the experimental results, as

shown in Figure 4b. Both experiment and numerical results show that with the increase of shear strains, the damping decreases.

Figure 4c compares the estimates of the initial shear stiffness at zero shear displacement for increasing values of the applied vertical displacement according to the numerical FE model and the experimental results.

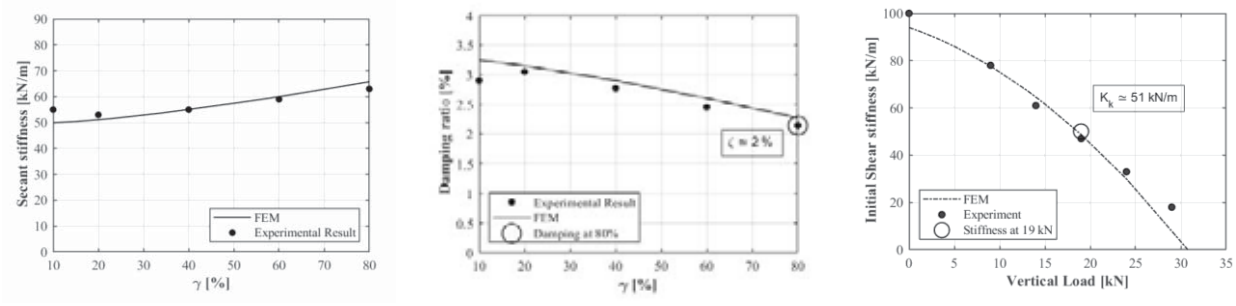

(a) (b) (c)

Figure 4: (a) Secant shear stiffness-average shear strain relation (b) Equivalent damping ratio at different levels of shear strain (c) Stiffness vs vertical displacement. Experimental values taken from [11].

The numerical model provides an overall good estimate of the shear stiffness for increasing of compression levels. In general, the horizontal stiffness reduces with the increase of the vertical load, and the condition of instability is attained when it becomes zero. It is noteworthy that the observed buckling load is 50% higher than the applied compression load of 19kN and it is also 3 times higher than the critical load evaluated according to the theory of Gent and of Koh and Kelly [15] [16]. It is also interesting to observe that the ratio between the initial horizontal and vertical stiffness is about 43, which is significantly lower than the values typical of high shape factor bearings ([1], e.g. about 800 for S=12 in Tubaldi et al. [17], which deals with isolation bearings for bridges).

3 SHAKING TABLE TESTS

3.1 Prototype and test description

This subsection describes the shaking table tests carried out at the Department of Structures for Engineering and Architecture of University of Naples Federico II on a prototype base-isolated building with LSF bearings [8]. The steel superstructure is composed of one level and has a total height of 2900mm. The plan dimensions of the structure are 2500x2000mm with concrete slab placed on the roof of the structure, having a depth of 25mm, and concrete blocks added to the base level to achieve a total mass M_{tot} = 7.7 tons. The columns have a box section 150x150x15mm. The beams of the top floor are pinned to the columns and are hot-formed square hollow sections 120x120x12.5mm. The four perimetric beams at the base of the frame have HEM 160 profile. The bearings are identical to those tested at TARRC. The same mock-up has been recently used for bi-directional tests on recycled rubber and fibre-reinforced unbounded isolators [18][19]. Ground motions were applied along the direction in which the frame span is 2500 mm. The vibration period of the fixed-base structure is T_s = 0.24 s. The isolation system of the scaled prototype was designed to achieve a horizontal vibration period T_{is} = 0.92 s, estimated from an assumed value of the rubber shear modulus of 0.5MPa and considering the superstructure as rigid and the bearings as infinitely stiff in the vertical direction. Under these simplifying assumptions, the isolation period can be expressed as $T_{is} = 2\pi\sqrt{(M_{tot}/K_{is})}$, where K_{is} is the total stiffness of the bearings in the horizontal direction. It is noteworthy that the system was designed considering a geometry scale factor of

1/3 and an elastic modulus scale factor of 1. Therefore, according to the dynamic similitude rule, the equivalent period of the full-scale structure is T_{fs} = 1.59 s, (i.e. $T_{fs} = \sqrt{3}T_{is}$). A set of seven waveforms was selected from the European strong-motion database, whose main characteristics are described in Table 2.

Waveform ID	Earthquake Name	Earthquake Country	Mw	PGA (m/s²)	PGV (cm/s)	PGD (cm)
7142	Bingol	Turkey	6.3	2.55	18.29	3.25
55	Friuli	Italy	6.5	2.55	15.25	9.29
200	Montenegro	Montenegro	6.9	2.55	12.87	9.60
428	Etolia	Greece	5.3	2.55	12.46	6.06
372	Lazio Abruzzo	Italy	5.9	2.55	15.02	6.80
290	Campano Lucano	Italy	6.9	2.55	44.10	16.20
287	Campano Lucano	Italy	6.9	2.55	43.90	14.00

Table 2: Ground motion characteristics (Mw=Magnitude, PGA=Peak ground acceleration, PGV= Peak ground velocity, PGD= Peak ground displacement)

3.2 Simulation of shaking table tests

Figure 5 shows the simplified FEM model of the isolated structure developed in SAP2000 [10]. The steel columns and beams of the frame are assumed to remain elastic and are modelled with beam elements assigning a Young's modulus of 210000MPa, a Poisson's ratio of 0.3, and mass density of 7.8E-09 ton/mm^3. The mass at top and bottom level is 2.05 and 1.8 tons respectively, so that the vertical load applied to the bearing is 19kN. The isolators are modelled using the two-node link linear elements [10] connecting the bottom of the base beam to the ground (Figure 5).

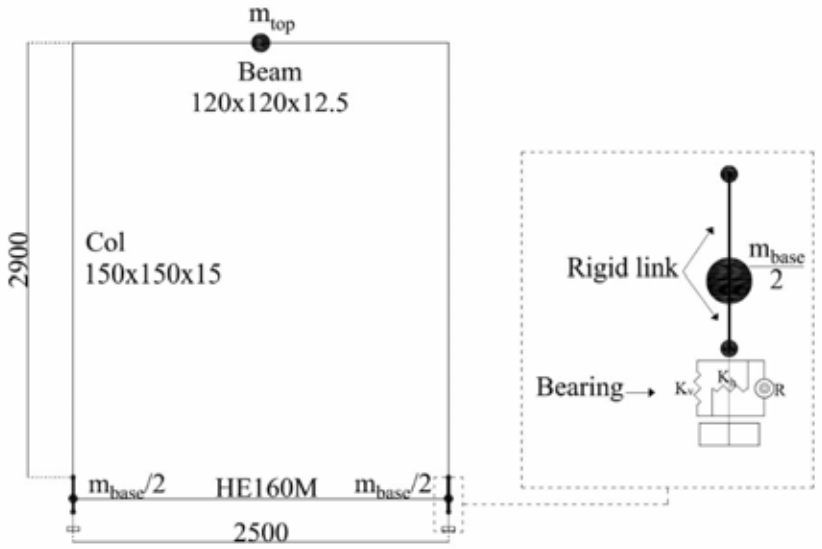

Figure 5: Front view of the base isolated structure configuration and detail of the isolation system

Table 3 shows the values of the stiffness assigned to the two-node link elements, where K_v, K_h and K_r are the vertical, shear and rotational stiffnesses, respectively. These values are de-

termined by considering the bearing model developed in Abaqus and applying a small axial displacement, shear displacement and rotation on the bearings compressed by a vertical load of 19 kN.

K_v	K_h	K_r
N/mm	N/mm	Nmm
2209	51	1180000

Table 3: Link Element Properties

A Rayleigh damping model has been assumed and the damping ratio of the first two modes of the base isolated structure has been set equal to $\zeta = 0.02$. In contrast to the definition of damping on a 3D numerical model, that is related to the material property, the damping ratio in this case needs to be specified to the whole bearing. The adopted value of ζ refers to the equivalent damping ratio of bearing correspondent to 80% of shear strain, shown in Figure 4b. Seismic analyses are performed using the developed model. Displacement history of isolator and top structure horizontal accelerations resulting from numerical model are compared to the recorded ones for Etolia earthquake input, as shown in Figure 6a-b. In general, it can be observed that assuming a linearized behaviour of the bearings superimposed on the finite strains induced by the vertical static loading on the bearing provides a good approximation of the response in the case of Etolia earthquake input.

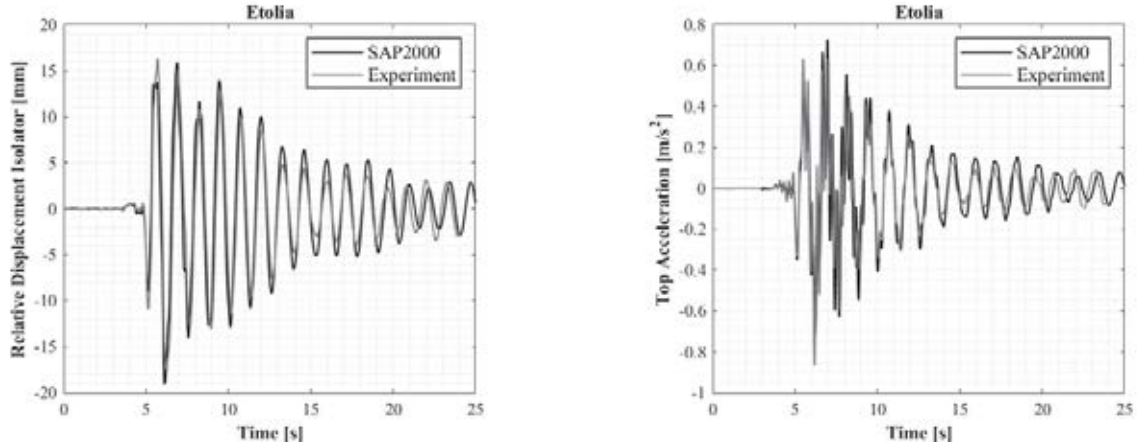

(a) (b)

Figure 6: (a) Relative Displacement Isolator time history (b) Acceleration at the top of the superstructure

Table 4 shows the numerical-experimental comparisons in terms of maximum absolute values of the isolator deflection, interstorey drift and acceleration at the top of the structure. The response of the superstructure is slightly underestimated, and this may be due to the assumption of a rigid connection between the columns and the base.

Earthquake Name	**Max Displacement Isolator [mm]**			**Max Drift Structure [%]**			**Max Top Acceleration [m/s²]**		
	Exp	SAP 2000	Relative error %	Exp	SAP 2000	Relative error %	Exp	SAP 2000	Relative error %
Bingol	45.88	36.37	-20.73	0.30	0.30	0.56	1.22	1.22	-0.16
Friuli	17.24	16.08	-6.73	0.17	0.13	-24.49	0.87	0.68	-21.68
Montenegro	17.29	18.88	9.20	0.17	0.14	-20.08	0.86	0.72	-16.47
Etolia	17.41	19.03	9.30	0.17	0.14	-17.71	0.86	0.73	-15.87

Earthquake Name	Max Displacement Isolator [mm]			Max Drift Structure [%]			Max Top Acceleration [m/s^2]		
	Exp	SAP 2000	Relative error %	Exp	SAP 2000	Relative error %	Exp	SAP 2000	Relative error %
Bingol	45.88	36.37	-20.73	0.30	0.30	0.56	1.22	1.22	-0.16
Friuli	17.24	16.08	-6.73	0.17	0.13	-24.49	0.87	0.68	-21.68
Lazio/Abruzzo	17.55	19.03	8.43	0.16	0.14	-14.33	0.87	0.73	-16.01
ID 290	17.57	18.95	7.85	0.16	0.14	-16.85	0.87	0.73	-15.61
ID 287	17.33	18.94	9.29	0.17	0.14	-20.24	0.86	0.72	-16.02

Table 4 Maximum absolute values of various response parameters according to experimental test and numerical model.

4 CONCLUSION AND FUTURE RESEARCH NEEDS

This study investigates numerically the mechanical behaviour of elastomeric bearings with low shape factor (LSF) under compressive and shear loading, and the dynamic behaviour of structures mounted on them. The first part of the paper illustrates the development of a three-dimensional (3D) numerical model in Abaqus for simulating the experimental tests conducted at Tun Abdul Razak Research Center (TARRC) rubber research center on LSF rubber bearings with low damping. It is shown that the Yeoh hyperelastic material model, calibrated against material double-shear tests, can be used to accurately describe the complex nonlinear shear response of compressed LSF bearings.

In the second part of the paper, the shaking table tests carried out on a model isolated structure on LSF bearings performed at University of Naples Federico II are simulated using a simplified numerical model. The prototype isolated structure is analyzed using SAP2000 under different earthquake loadings and the numerical estimates of the response are compared with the experimental ones. The isolators are described using two-node links with linear elastic behaviour and vertical, shear and rotational stiffnesses are estimated by performing numerical analyses of the LSF bearing in Abaqus. In general, it is observed that the development of simple FEM model for the tested prototype isolated structure can be used for preliminary assessment and design purposes due to the good agreement between numerical responses and experimental results.

Further studies will include the development of advanced numerical models to evaluate the behaviour of LSF bearings and their capability of providing full three-dimensional isolation. Moreover, the response of LSF bearing made with high damping rubber compounds, characterized by more complex behaviour, will be investigated.

REFERENCES

[1] J. M. Kelly and D. A. Konstantinidis, *Mechanics of Rubber Bearings for Seismic and Vibration Isolation*. 2011.

[2] M. C. Constantinou, A. Kartoum, and J. M. Kelly, “Analysis of compression of hollow circular elastomeric bearings,” *Eng. Struct.*, vol. 14, no. 2, pp. 103–111, 1992.

[3] G. M. Montuori, E. Mele, G. Marrazzo, G. Brandonisio, and A. De Luca, “Stability issues and pressure–shear interaction in elastomeric bearings: the primary role of the secondary shape factor,” *Bull. Earthq. Eng.*, vol. 14, no. 2, pp. 569–597, 2016.

[4] E. Tubaldi, S. A. Mitoulis, H. Ahmadi, and A. Muhr, "A parametric study on the axial behaviour of elastomeric isolators in multi-span bridges subjected to horizontal seismic excitations," *Bull. Earthq. Eng.*, vol. 14, no. 4, pp. 1285–1310, 2016.

[5] J. M. Kelly, "Base Isolation in Japan," no. December, p. 100, 1988.

[6] I. D. Aiken, J. M. Kelly, and F. F. Tajirian, "Mechanics of Low Shape Factor Elastomeric Seismic Isolation."

[7] F. Cilento, R. Vitale, M. Spizzuoco, G. Serino, and A. H. Muhr, "Analysis of the Experimental Behaviour of Low Shape Factor Isolation Rubber Bearings by Shaking Table Investigation," 2017.

[8] F. Cilento, R. Vitale, M. Spizzuoco, G. Serino, and A. Muhr, "Dynamic behaviour in compression and shear of low shape factor rubber blocks," *Ing. Sismica*, vol. 36, no. 2, pp. 86–102, 2017.

[9] "Dassault Systèmes, Abaqus Analysis User's Manual Version 2018."

[10] C. CSI, "SAP2000 Integrated Software for Structural Analysis and Design," Computers and Structures Inc., Berkeley, "No Title."

[11] G. Cuomo, "Design, development and experimental validation of multilayer modular laminated natural rubber isolators.," 2014.

[12] R. . Ogden, "Dover Civil and Mechanical Engineering R. W. Ogden - Non-Linear Elastic Deformations." 1984.

[13] H. R. Ahmadi, J. G. R. Kingston, and A. H. Muhr, "Dynamic Properties of Filled Rubber — Part I: Simple Model, Experimental Data and Simulated Results," *Rubber Chem. Technol.*, vol. 81, no. 1, pp. 1–18, 2008.

[14] J. Bergstrom, "Constitutive modeling of the large strain time-dependent behavior of elastomers," vol. 46, no. 5, p. 931, 1998.

[15] C. G. Koh and J. M. Kelly, "Modelling of seismic isolation bearings including shear deformation and stability effects," *Appl. Mech. Rev.*, vol. 42, no. 11, pp. 113–120, 1989.

[16] A. N. Gent, "Elastic Stability of Rubber Compression Springs," *Rubber Chem. Technol.*, vol. 38, no. 2, pp. 415–430, 1965.

[17] E. Tubaldi, S. A. Mitoulis, and H. Ahmadi, "Comparison of different models for high damping rubber bearings in seismically isolated bridges," *Soil Dyn. Earthq. Eng.*, vol. 104, no. May 2017, pp. 329–345, 2018.

[18] D. Losanno, M. Spizzuoco, and A. Calabrese, "Bidirectional shaking-table tests of unbonded recycled-rubber fiber-reinforced bearings (RR-FRBs)," *Struct. Control Heal. Monit.*, vol. 26, no. 9, 2019.

[19] D. Losanno, I. E. Madera Sierra, M. Spizzuoco, J. Marulanda, and P. Thomson, "Experimental performance of unbonded polyester and carbon fiber reinforced elastomeric isolators under bidirectional seismic excitation," *Eng. Struct.*, vol. 209, no. November 2019, p. 110003, 2020.